On the Magnetization of Ferromagnetic Crystals

FRANCIS BITTER, *Westinghouse Research Laboratories*
(Received December 15, 1932)

In a previous article a function E_θ is discussed. This function gives the energy of a crystal as a function of the direction of magnetization. The present paper contains photographs of plaster models representing E_θ for an undistorted crystal of nickel, for an undistorted crystal of iron in zero applied field, and in a field of 100 oersteds parallel to the [100], [110], and [111] axes respectively, and for an iron crystal distorted by compression and extension along the above mentioned axes. Assuming that a crystal is magnetized to saturation in the direction in which E_θ has a minimum, magnetization curves for crystals distorted as mentioned above are calculated and illustrated.

IN a previous article[1] a procedure was outlined for describing some properties of strained ferromagnetic crystals. It is proposed to discuss the consequences of this procedure in greater detail. In the following pages certain aspects of magnetization are taken up.

PROCEDURE

Let i, j, k be subscripts denoting measurement along three axes parallel to the tetragonal axes of a cubic ferromagnetic crystal whose spontaneous magnetization is I_w. The orientation of I_w is given by the direction cosines α_i, α_j, α_k. The crystal may be distorted and the distortion described by the components of a strain tensor, A_{ij}. The energy for an arbitrary direction of magnetization is assumed to be:—

$$E_\theta = c\sum{}'\alpha_i^2\alpha_j^2 + K_1\sum A_{ii}\alpha_i^2 + K_2\sum{}'A_{ij}\alpha_i\alpha_j - I_w\sum\alpha_i H_i + \text{const.} \quad (1)$$

From this expression it is possible to calculate the magnetostriction in an arbitrary direction β_i, β_j, β_k.

$$\delta l/l = \chi_0 + \chi_1\sum\alpha_i^2\beta_i^2 + \chi^2\sum{}'\alpha_i\alpha_j\beta_i\beta_j. \quad (2)$$

The constants involved in Eq. (2) are related to those in Eq. (1).

$$\chi_1 = -K_1/(c_{11}-c_{12}); \quad \chi_2 = -K_2/2c_{44}. \quad (3)$$

The quantities c_{11}, c_{12}, c_{44} are the elastic constants of the cubic crystal under discussion. It is further assumed that the actual direction of magnetization of the crystal for any given set of external conditions is that direction in which E_θ has a minimum. If E_θ has minima in two or more directions ambiguities may arise.

EVALUATION OF CONSTANTS

For nickel[2] the constant c is approximately -2.5×10^4 ergs/cc and $I_w = 500$. For iron all the constants may be evaluated with sufficient accuracy to give some idea of the predictions of Eq. (1). From observations by Honda and Masiyama[3] we can evaluate χ_0, χ_1, and χ_2, as has been done in a previous article.[1] Certain constants, s_{11}, etc., related to the above elastic constants, c_{11}, etc., by the following equations:

$$c_{11} = s_{11} + s_{12}/(s_{11}+2s_{12})(s_{11}-s_{12}),$$
$$c_{12} = -s_{12}/(s_{11}+2s_{12})(s_{11}-s_{12}),$$
$$c_{44} = 1/s_{44},$$

were measured for iron by Goens and Schmid.[4] From their measurements we obtain $c_{11} = 0.237\times10^{13}$; $c_{12} = 0.141\times10^{13}$; and $c_{44} = 0.116\times10^{13}$ ergs/cc. Knowing the magnetostriction and the elastic constants, we may with the help of Eq. (3) evaluate K_1 and K_2. The constant c for iron is taken from Akulov.[5] The values of the various constants of Eq. (1) for iron as used in this paper

[1] F. Bitter, Phys. Rev. **42**, 697 (1932).

[2] F. Bitter, Phys. Rev. **38**, 546 (1931).

[3] K. Honda and Y. Masiyama, Sci. Rep. Tohoku Univ. **15**, 755 (1926).

[4] E. Goens and E. Schmid, Naturwiss. **19**, 520 (1931).

[5] N. Akulov, Zeits. f. Physik **57**, 249 (1929); **67**, 794 (1931).

are: $c=2.15\times 10^5$; $K_1=-3.06\times 10^7$; $K_2=2.85\times 10^7$ ergs/cc; $I_w=1718$.

THE REPRESENTATION OF E_θ

It is difficult to visualize the properties of the function E_θ without a rather wearisome lot of computing. Since E_θ promises to be of importance in the study of ferromagnetism, and perhaps also in the study of certain non-ferromagnetic crystals,[6] I have thought it worth the trouble to make a few models for representative values of the parameters involved. Various methods of representation are, of course, possible. Spherical polar coordinates were chosen. Thus, since E_θ defines an energy for any direction, we may represent E_θ by a surface surrounding a certain point in such a way that the length of the radius vector to the surface in any given direction is equal to E_θ for that direction. The disadvantage of this representation is that negative radii are not desirable. The arbitrary constant in Eq. (1) is therefore so chosen that the figure has a reasonable size and does not become negative. In other words, the length of the radius of the model is not proportional to the corresponding energy, but the difference in length between any two radii is proportional to the difference between the two corresponding energies.

The particular conditions illustrated below were chosen in such a way as to cover the most important aspects of the problem. The intention is to show what shapes the function E_θ may assume rather than to carry out the calculations for cases of experimental importance. This is especially apparent below when we speak of elastic compressions of 50 percent, etc., which are, of course, not experimentally realizable.

The first term in Eq. (1) contains only one parameter c, giving rise to two different types of material, one, like iron, for which $c>0$, and another, like nickel, for which $c<0$. The remaining terms in Eq. (1) represent the influence of crystal distortion and of an externally applied magnetic field. We shall consider these last terms only for a crystal of iron, and only for the six special cases listed in Table I.

It is to be observed that we have chosen distortions which give rise to no volume change.

TABLE I. *The parameters used in the illustrations of E_θ. H is the magnetic field, and e is the elongation.*

$H \parallel [100]$	$H_i=H;\ H_j=H_k=0$
$H \parallel [110]$	$H_i=H_j=H/2^{\frac{1}{2}};\ H_k=0$
$H \parallel [111]$	$H_i=H_j=H_k=H/3^{\frac{1}{2}}$
$e \parallel [100]$	$A_{ii}=e;\ A_{jj}=A_{kk}=-e/2;\ A_{ij}=A_{jk}=\cdots=0$
$e \parallel [110]$	$A_{ii}=A_{jj}=e/4;\ A_{kk}=-e/2;\ A_{ij}=A_{ji}=3e/4;\ A_{jk}=\cdots=0$
$e \parallel [111]$	$A_{ii}=A_{jj}=A_{kk}=0;\ A_{ij}=A_{ji}=A_{jk}=\cdots=e/2$

These distortions are not produced by the application of ordinary tension or compression. On the other hand the results obtained will be very similar to those resulting from true tension and compression, and in addition are particularly simple to calculate.

THE FUNCTION E_θ

Figs. 1 and 2 represent the function E_θ for the special case $A_{ii}=A_{ij}=\cdots=0$, $H=0$, i.e., for the undisturbed ideal lattice. Since the constant c for nickel is not only negative, but also ten times smaller than for iron, Fig. 1, if constructed on the same scale as Fig. 2, would not deviate much from sphericity. The scale used for Fig. 1 is such that 1 cm represents 1718/500 times as many ergs as a like distance in Fig. 2. Since the ratio 1718/500 is that of the saturation intensities, the scale chosen is such that a field H produces the same effect on the model for iron as on the model for nickel. In all the photographs here reproduced the plaster model stands next to a crystal model. In every case the axes of adjacent models are parallel. From Fig. 1 we see that in nickel E_θ has maxima in the direction of the tetragonal [100] axes, and minima in the direction of the trigonal [111] axes, whereas in iron, as shown in Fig. 2, the maxima and minima are reversed. In Figs. 3, 4, and 5 we have E_θ for iron in a field of 100 oersteds parallel to the [100], [110], and [111] axes respectively. In Figs. 6, 7, 8 and 9 are illustrated the effect of compression and elongation on E_θ in the absence of a magnetic field. Figs. 8 and 9 are two views of the same set of figures. Referring to Table I, compression corresponds to $e<0$, elongation corresponds to $e>0$. In the photographs the model on the left represents $e>0$, or elongation and the model on the right $e<0$, or compression. The stick resting on the crystal model in the center of each illustration

[6] F. Bitter, Phys. Rev. **42**, 731 (1932).

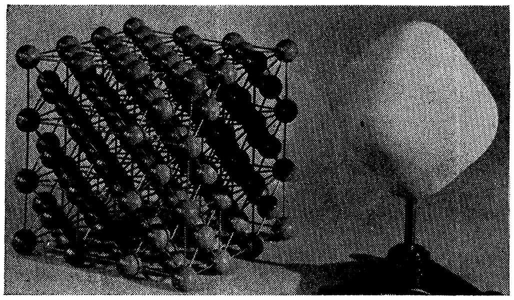

FIG. 1. E_θ for an undistorted nickel crystal.

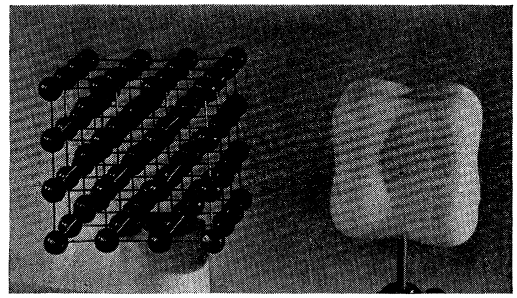

FIG. 2. E_θ for an undistorted iron crystal.

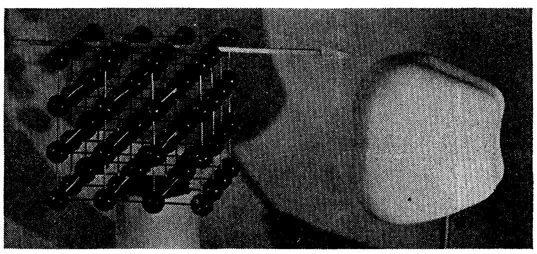

FIG. 3. E_θ for an iron crystal in a field of 100 oersteds parallel to a [100] axis.

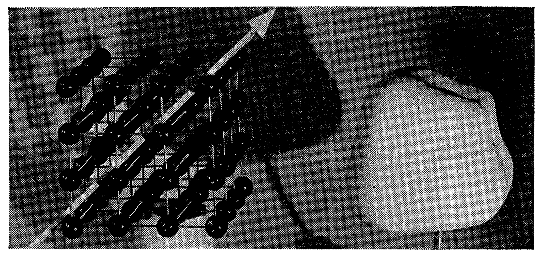

FIG. 4. E_θ for an iron crystal in a field of 100 oersteds parallel to a [110] axis.

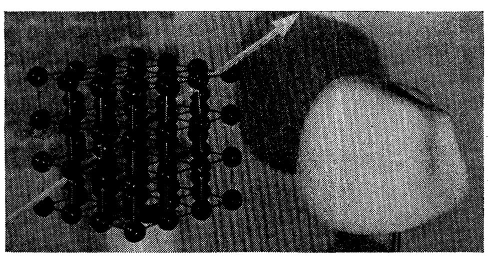

FIG. 5. E_θ for an iron crystal in a field of 100 oersteds parallel to a [111] axis.

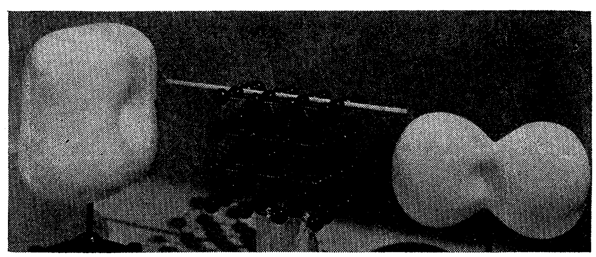

FIG. 6. On the left, E_θ for an iron crystal elastically stretched 1 percent along a [100] axis. On the right, E_θ for an iron crystal elastically compressed 1 percent along a [100] axis.

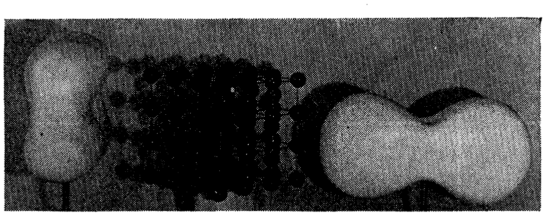

FIG. 7. On the left, E_θ for an iron crystal elastically stretched 1 percent along a [110] axis. On the right, E_θ for an iron crystal elastically compressed 1 percent along a [110] axis.

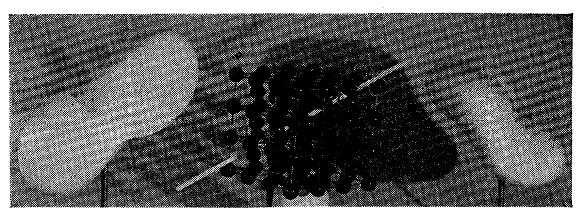

FIG. 8. On the left, E_θ for an iron crystal elastically stretched 1 percent along a [111] axis. On the right, E_θ for an iron crystal elastically compressed 1 percent along a [111] axis.

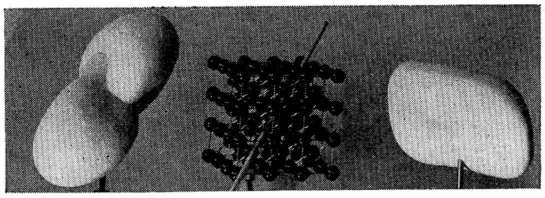

FIG. 9. A second view of the models shown in Fig. 8.

represents the direction of elongation or contraction. The models were all made for $e=\pm 0.01$. All the models in Figs. 2–9 are made on precisely the same scale except the model on the left of Fig. 6. For this model a slightly larger additive constant was used to avoid negative values of E_θ. The models in Fig. 6 depend only on c and K_1, while those in Figs. 8 and 9 depend only on c and K_2, as may readily be verified by substituting the values listed in Table I into Eq. (1). Because K_1 and K_2 in iron have opposite signs compression along a [100] axis has an effect on E_θ similar to extension along a [111] axis. Further, as has already been pointed out,[1] E_θ for compression along a digonal [110] axis depends on K_2, K_1+K_2, and K_1-K_2.

Magnetization

The magnetization curves obtained by applying a field parallel to the elongation or compression in Figs. 6, 7, 8 and 9 are shown in Figs. 10, 11 and 12. The cross-hatched portions of the curves indicate that there is a transition from one minimum of E_θ to another, and that we therefore have a transition in some unspecified manner from one magnetization curve to another. Some of the magnetization curves are vertical for $H=0$. These vertical portions also involve transitions from one minimum of E_θ to another. Experimental evidence already presented[5] indicates that for $e=0$, the curves as drawn represent the behavior of actual iron crystals fairly well. As far as I know, no experimental data exist with which to check the other curves.

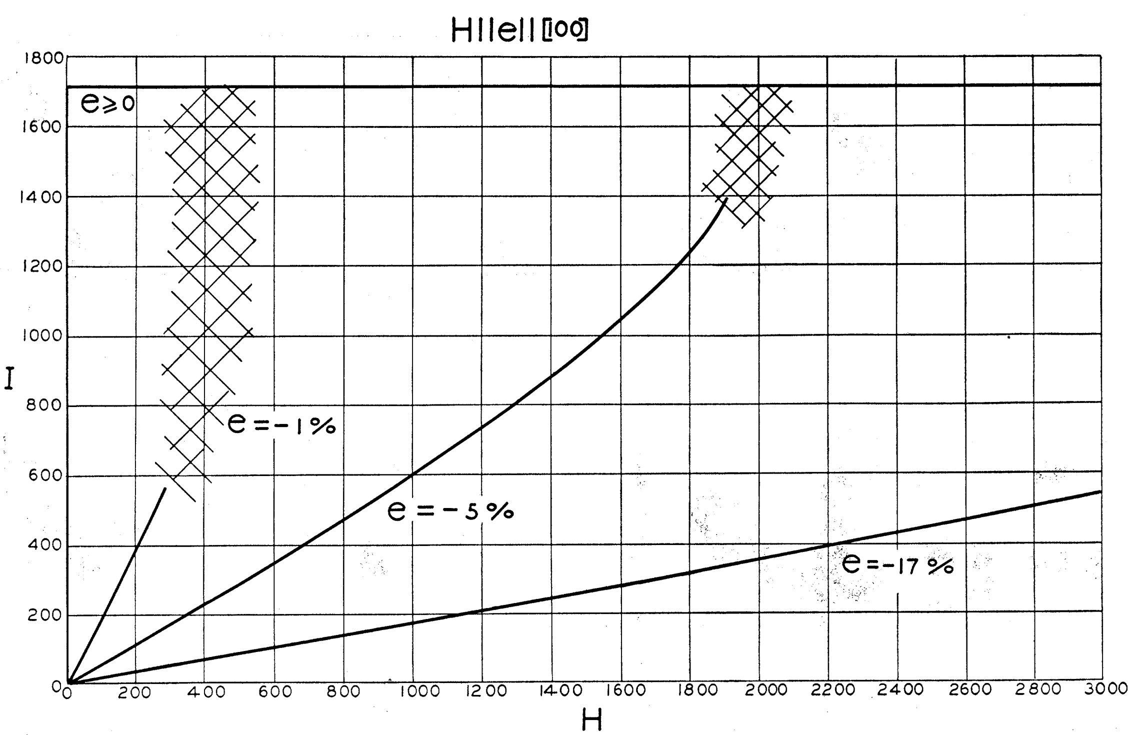

FIG. 10. Magnetization curves for an iron crystal elastically stretched or compressed along a [100] axis by an amount e, the applied magnetic field being parallel to the compression.

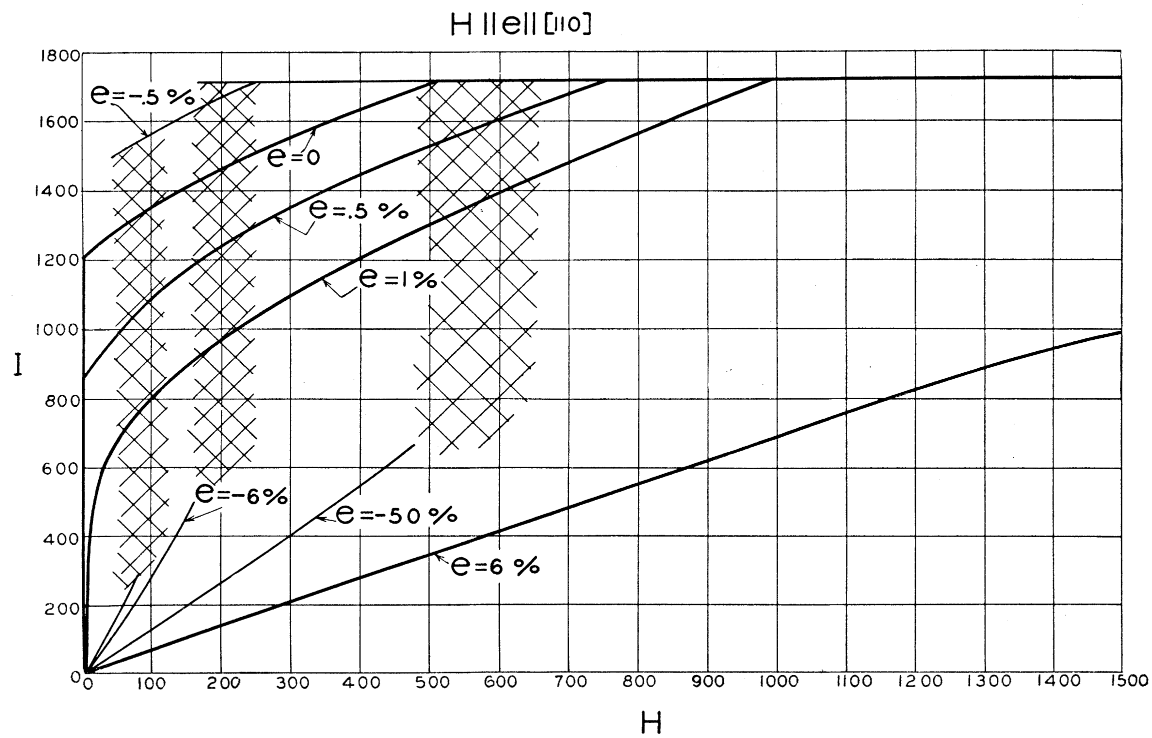

FIG. 11. Magnetization curve for an iron crystal elastically stretched or compressed along a [110] axis by an amount *e*, the applied magnetic field being parallel to the elongation.

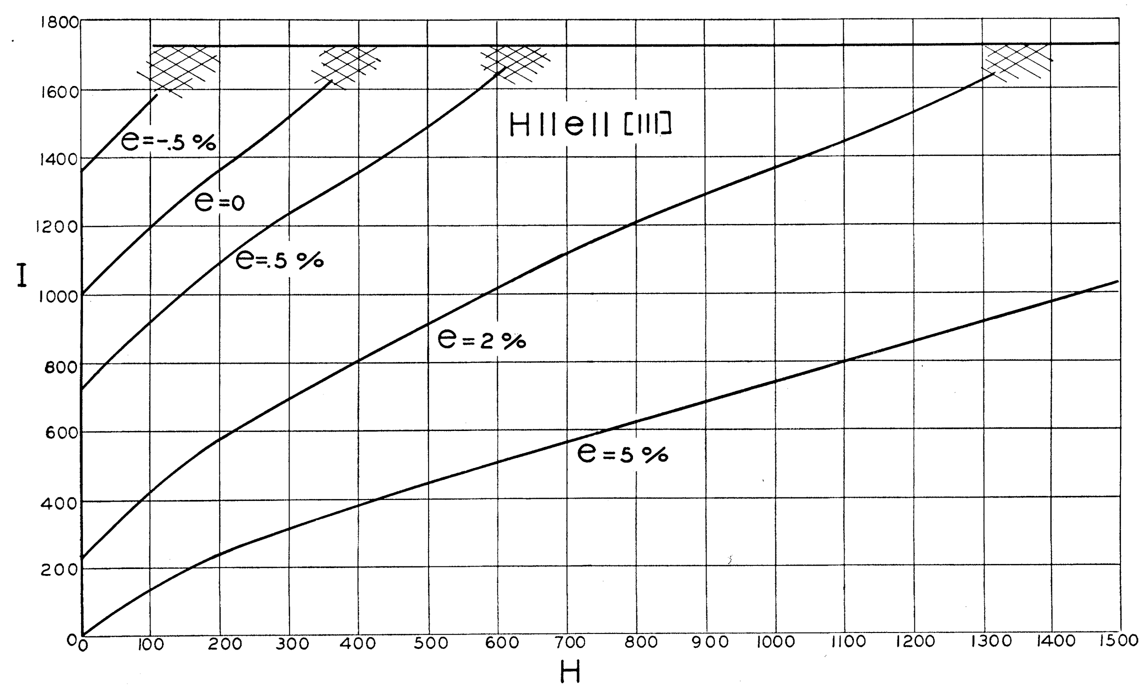

FIG. 12. Magnetization curve for an iron crystal elastically stretched or compressed along a [111] axis by an amount *e*, the applied magnetic field being parallel to the compression.

The formulae derived from Eq. (1) representing the curves drawn in Figs. 10–12 are:

e|| [*100*]—*Fig. 10.*

$$H=aI+bI^3,\quad a=(3eK_1+4c)/I_w^2,\quad b=-8c/I_w^4. \tag{4}$$

e|| [*110*]—*Fig. 11.*

For $e>0$ and for the upper portion of the curve for which $e=-0.005$

$$H=aI+bI^3,\quad a=(3eK_2-4c)/I_w^2,\quad b=8c/I_w^4, \tag{5}$$

for the lower part of the curves corresponding to $e<0$

$$H=aI+bI^3,\quad a=[(3/2)(K_1+K_2)e+4c]/I_w^2,\quad b=-6c/I_w^4. \tag{6}$$

The shape of E_θ should be examined in some detail before applying this formula for small values of e.

e|| [*111*]—*Fig. 12.*

$$H=\frac{3^{\frac{1}{2}}}{I_w}\,\frac{2c\sin\theta\cos\theta[2\cos^2\theta-\sin^2\theta]+eK_2[\sin\theta\cos\theta+2(\cos^2\theta-\sin^2\theta)]}{-\sin\theta+2^{\frac{1}{2}}\cos\theta},$$
$$I=I_w[(1/3^{\frac{1}{2}})\cos\theta+(2/3)^{\frac{1}{2}}\sin\theta]. \tag{7}$$

Anyone interested in securing casts of the plaster models here illustrated should communicate with the Magnetic Division of the Westinghouse Research Laboratories, East Pittsburgh, Pennsylvania.

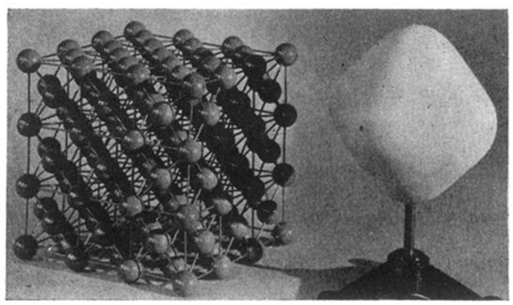

FIG. 1. E_θ for an undistorted nickel crystal.

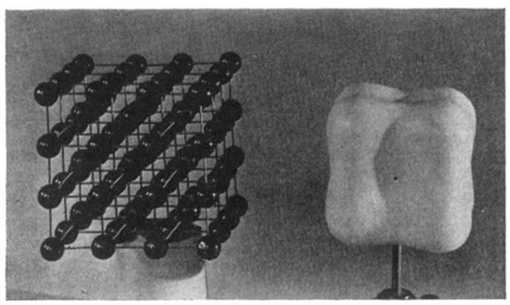

FIG. 2. E_θ for an undistorted iron crystal.

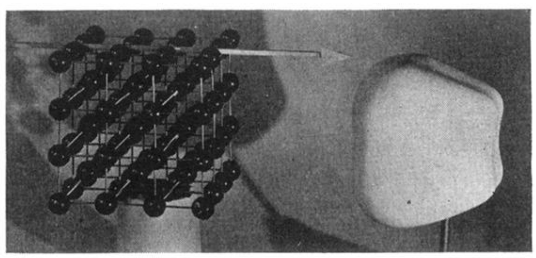

FIG. 3. E_θ for an iron crystal in a field of 100 oersteds parallel to a [100] axis.

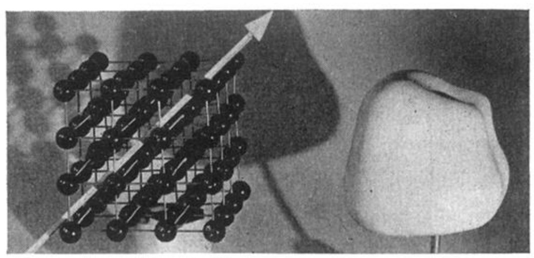

FIG. 4. E_θ for an iron crystal in a field of 100 oersteds parallel to a [110] axis.

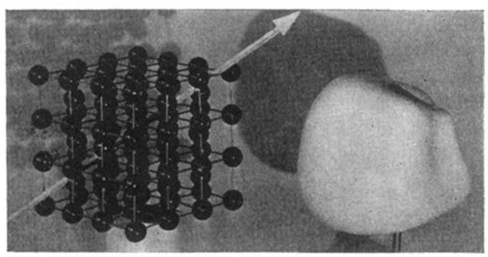

FIG. 5. E_θ for an iron crystal in a field of 100 oersteds parallel to a [111] axis.

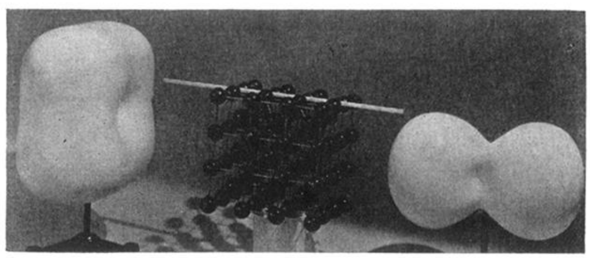

FIG. 6. On the left, E_θ for an iron crystal elastically stretched 1 percent along a [100] axis. On the right, E_θ for an iron crystal elastically compressed 1 percent along a [100] axis.

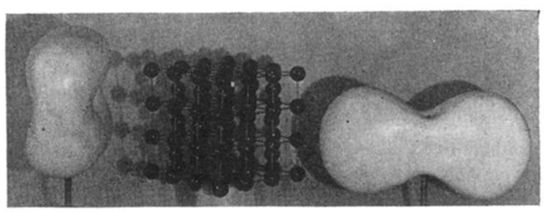

FIG. 7. On the left, E_θ for an iron crystal elastically stretched 1 percent along a [110] axis. On the right, E_θ for an iron crystal elastically compressed 1 percent along a [110] axis.

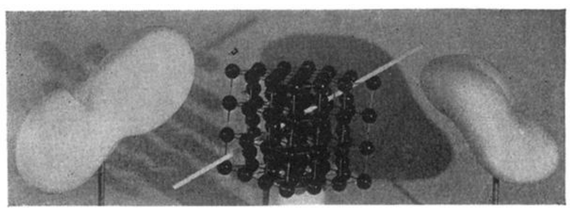

FIG. 8. On the left, E_θ for an iron crystal elastically stretched 1 percent along a [111] axis. On the right, E_θ for an iron crystal elastically compressed 1 percent along a [111] axis.

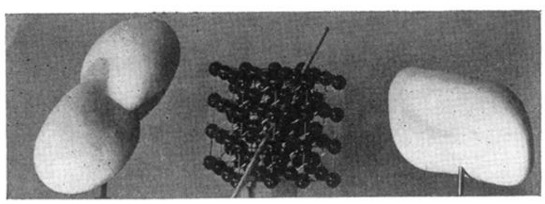

FIG. 9. A second view of the models shown in Fig. 8.